

Supporting Information

Blending block copolymer micelles in solution; Obstacles of blending.

Daniel B. Wright,[†] Joseph P. Patterson,[‡] Nathan C. Gianneschi,[‡] Christophe Chassenieux,[‡]
Olivier Colombani,[‡] and Rachel K. O'Reilly^{†*}

[†] University of Warwick, Department of Chemistry, Gibbet Hill Road, Coventry CV4 7AL,
UK.

[‡] LUNAM Université, Université du Maine, IMMM UMR CNRS 6283, Département PCI,
Avenue Olivier Messiaen, 72085 Le Mans Cedex 09, France.

[‡] Department of Chemistry & Biochemistry, University of California, 9500 Gilman Drive, La
Jolla, San Diego, CA, USA.

Contents

Methods and Materials.....	3
Characterization methods.....	3
¹ H Nuclear magnetic resonance	3
Size exclusion chromatography	3
Differential scanning calorimetry	3
Refractive index increment	3
Laser light scattering (LLS)	4
Dynamic light scattering (DLS).....	4
Static light scattering (SLS)	5
Cryogenic transmission electron microscopy samples (cryo-TEM).....	6
Reactivity ratios of the DMA/EHA and DMA/IBA comonomers.....	7
Characteristics of the P(DMA- <i>co</i> -EHA) and P(DMA- <i>co</i> -IBA) copolymers	8
Molar mixing ratios for the blended block copolymers systems.	8
Laser light scattering analysis of the parent polymers	9
Variable temperature ¹ H NMR spectroscopy.....	11
Dynamic light scattering of blends formed from 5	15
Cryo-TEM analysis of 8	16
REFERENCES	16

Methods and Materials

Characterization methods

¹H Nuclear magnetic resonance

¹H Nuclear magnetic resonance (NMR) spectra were recorded on a Bruker DPX-400 spectrometer in CDCl₃ or D₂O. Chemical shifts are given in ppm downfield from tetramethylsilane TMS.

Size exclusion chromatography

Size exclusion chromatography (SEC) measurements were performed on a set of two PLgel 5 μm Mixed-D columns with HPLC grade solvents (Fisher) as eluents: dimethylformamide (DMF) with 1.06 g/L of LiCl at 40 °C at a flow rate of 1 mL/min or chloroform (CHCl₃) with 2.5% volume of NEt₃ at 40 °C at a flow rate of 1 mL/min. The molecular weights of the synthesised polymers were calculated relative to poly(methyl methacrylate) (PMMA) and poly(styrene) (PS) standards from refractive index traces.

Differential scanning calorimetry

Differential scanning calorimetry (DSC) was carried out in an aluminium sample holder with an empty aluminium pan as the reference. Changes in heat flow were recorded between -100 °C and 150 °C over two cycles with a scan rate of 5 °C /min under a nitrogen atmosphere. Calibration was achieved using indium metal standards supplied by Mettler Toledo.

Refractive index increment

The specific refractive index increment (dn/dC) of the polymers in water was measured on a refractometer (Bischoff RI detector) operating at a wavelength of 632 nm.

Laser light scattering (LLS)

Measurements were performed at angles of observation ranging from 20° up to 130° with an ALV CGS3 setup operating at $\lambda_0 = 632$ nm and at 20 °C \pm 1 °C. Data were collected in duplicate with 240 s run times. Calibration was achieved with filtered toluene and the background was measured with filtered solvent (NaCl 0.1 M solution).

Dynamic light scattering (DLS)

The normalized intensity autocorrelation functions $g_2(t)$ obtained from dynamic light scattering were related to $g_1(t)$ (the normalized electric field autocorrelation functions) *via* the so-called Siegert relation. Then $g_1(t)$ were analyzed in terms of a continuous distribution of relaxation times (eqn. S1) using the REPES routine¹ without assuming a specific mathematical shape for the distribution of the relaxation times ($A(\tau)$).

$$g_1(t) = \int_0^{\infty} A(\tau) \exp(-t/\tau) d\tau \quad (\text{S1})$$

When comparing micelle distributions directly to one another the Gauss-Gex routine was used.²

The apparent diffusion coefficient D was calculated from eqn. S2 given that the z-average relaxation rates τ of the scatterers were q^2 -dependent, where q is the scattering vector given by $q = (4\pi n/\lambda_0) \cdot \sin(\theta/2)$ with θ the angle of observation and $n = 1.333$ the refractive index of the solvent (water).

$$D = 1/\tau q^2 \quad (\text{S2})$$

The concentration dependence of D is given by $D = D_0(1+k_D C)$ where k_D is the dynamic second virial coefficient and D_0 the diffusion coefficient used for computing the

hydrodynamic radius (R_h) of the scatterers according to the Stokes-Einstein equation (eqn. S3). Here, measurements were performed only at $C = 2.5$ g/L giving D at this concentration only. However, interactions could be neglected here at least for solutions of **1-3** at equilibrium so that $D_{2.5 \text{ g/L}} \sim D_0$.

$$D_0 = \frac{kT}{6\pi\eta R_h} \quad (\text{S3})$$

With η the solvent viscosity, k Boltzmann's constant and T the absolute temperature.

Static light scattering (SLS)

The Rayleigh ratio of the solutions have been measured using toluene as a reference according to: $R_\theta = R_{\text{tol}} \cdot (I_{\text{solution}}(\theta) - I_{\text{solvent}}(\theta)) / I_{\text{toluene}}(\theta)$ where I_i represents the intensity scattered by species i and R_{tol} is the Rayleigh ratio of the reference. We use typically $R_{\text{tol}} = 1.35 \times 10^{-5} \text{ cm}^{-1}$ the Rayleigh ratio of toluene for a wavelength $\lambda_0 = 632.8$ nm. In dilute solutions if $R_g \cdot q < 1$ where R_g is the radius of gyration, the q and concentration dependence of R_θ is given by: (eqn S4).

$$\frac{KC}{R_\theta} = \frac{1}{M_{\text{app}}} \left(1 + \frac{q^2 R_g^2}{3} \right) \quad (\text{S4})$$

Where M_{app} is the apparent weight average molecular weight. M_{app} is in principle affected by interactions, but at 2.5 g/L, the approximation could be made that $M_{\text{app}} \sim M_w$, the true molecular weight of the aggregates. K is an optical constant given by (eqn. S5):

$$K = \frac{4\pi^2 n_0^2}{\lambda^4 N_a} \left(\frac{dn}{dC} \right)^2 \quad (\text{S5})$$

Where $n_o = 1.496$ is the refractive index of the reference liquid (toluene), dn/dC is the specific refractive index increment determined by differential refractometry and N_A is Avogadro's number. Values of M_w were used to derive the aggregation number of the micellar aggregates $N_{agg} = M_{w,aggregate}/M_{w,unimers}$.

When in some cases two modes of relaxation were observed by DLS measurements, R_θ was described as the sum of a fast and a slow contribution according to (eqn. S6).

$$R_\theta = R_{\theta f} + R_{\theta s} \quad (S6)$$

Where f and s stand respectively for fast and slow and using equation S7. $R_{\theta f}$ could be calculated as:

$$R_{\theta f}(q) = \frac{A_f(q)}{(A_f(q) + A_s(q))} R_\theta \quad (S7)$$

Where A_f and A_s are the relative amplitudes of the fast and slow modes obtained by DLS. The slow mode of relaxation when observed can be attributed to spurious aggregates with a negligible weight fraction but larger scattering intensity.³⁻⁵ Consequently, only the fast mode was taken into account, assuming that the polymer concentration involved in the fast mode corresponded to the macroscopic polymer concentration.

Cryogenic transmission electron microscopy samples (cryo-TEM).

Cryo-TEM was conducted on a FEI Sphera microscope operated at 200 keV. 3.5 μ L of sample was added to freshly glow discharged Quantifoil R2/2 TEM grids. The grids were

blotted with filter paper under high humidity to create thin films and rapidly plunged into liquid ethane. The grids were transferred to the microscope under liquid nitrogen and kept at < -175 °C while imaging.

Reactivity ratios of the DMA/EHA and DMA/IBA comonomers

Table S1. f_1 and F_1 values for the copolymerisation of DMA (f_1) and EHA(f_2).

Experiment	Mol fraction in initial feed (f_1)	Mol fraction in copolymer (F_1)
1	84	81
2	60	63
3	45	48
4	40	41
5	30	27

Table S2. f_1 and F_1 values for the copolymerisation of DMA (f_1) and IBA(f_2).

Experiment	Mol fraction in initial feed (f_1)	Mol fraction in copolymer (F_1)
1	80	75
2	63	58
3	51	45
4	39	34
5	30	28

Characteristics of the P(DMA-*co*-EHA) and P(DMA-*co*-IBA) copolymers

Table S3. Thermal analysis of P(DMA_{1-x}-*co*-EHA_x)_m and P(DMA_{1-x}-*co*-IBA_x)_m copolymers.

Monomer	Polymer	x ^a	m ^a	Random Block
				T _g (°C) ^c
EHA	1	0.60	70	-18
	2	0.50	69	-5
	3	0.40	71	8
IBA	7	0.60	68	88
	8	0.50	71	90
	9	0.40	66	87

^a Determined by ¹H NMR spectroscopy (see Figure 1 for details). ^b Determined by end-group analysis from ¹H NMR spectroscopy (see Figure 1 for details). ^c Determined by differential scanning calorimetry. T_g(PDMA) = 85 °C,⁶ T_g(PEHA) = -60 °C,⁷ T_g(PIBA) = 90 °C.⁸

Molar mixing ratios for the blended block copolymers systems.

Table S4. Molar mixing ratios and assembly pathway for the blended block copolymer systems **1 - 3**.

Blended diblock copolymer	Pathway	Mole fraction	Mole fraction	Theoretical EHA in core block (mol%)
		1	3	
B-TF-2	TF	0.50	0.50	50%
B-DD-2	DD	0.50	0.50	50%
B-SS-2	SS	0.50	0.50	50%

Table S5. Molar mixing ratios and assembly pathway for the blended block copolymer systems **4 - 6**.

Blended diblock copolymer	Pathway	Mole fraction 4	Mole fraction 6	Theoretical EHA in core block (mol%)
B-TF-5	TF	0.50	0.50	80%
B-DD-5	DD	0.50	0.50	80%
B-SS-5	SS	0.50	0.50	80%

Table S6. Molar mixing ratios and assembly pathway for the blended block copolymer systems **7 - 9**.

Blended diblock copolymer	Pathway	Mole fraction 7	Mole fraction 9	Theoretical IBA in core block (mol%)
B-TF-8	TF	0.50	0.50	50%
B-DD-8	DD	0.50	0.50	50%
B-SS-8	SS	0.50	0.50	50%

Laser light scattering analysis of the parent polymers

Table S7. Laser light scattering analysis of **1**, **3**, **7** and **9** at room temperature before and after heating.

Diblock copolymer	Pathway	N_{agg}	R_h (nm)	N_{agg} After Heating	R_h (nm) After Heating
P-TF-1	TF	604	60	102	16
P-DD-1	DD	166	30	97	17
P-SS-1	SS	95	18	95	18
P-TF-3	TF	45	17	42	14
P-DD-3	DD	33	15	45	15
P-SS-3	SS	38	14	38	14
P-DD-7	DD	547	55	547	55
P-SS-7	SS	98	14	98	14
P-DD-9	DD	154	25	154	25
P-SS-9	SS	63	14	63	14

The pathway-dependency of the characteristics of the aggregates is a clear indication that these structures are out of equilibrium at room temperature. Note that the pathway dependency is stronger for higher contents of hydrophobic monomer (see **1** vs. **3** for example). As a consequence, the strong pathway-dependency of sample **1** will dominate the

response of the system in light scattering for out-of-equilibrium mixtures of **1+3** at room temperature, explaining why the pathway-dependency is stronger for mixtures of **1+3** than for pure **2** before equilibration.

Using equations S8 a weight average N_{agg} value for non-blended micelles, that is for a mixture of micelles of two different types respectively consisting of only one of the two polymers in the blend can be calculated (using mass concentrations). This value can then be compared to the experimentally obtained blend value to understand if indeed the micelles formed are blends (micelles consisting of the two types of polymers) formed from the two parent polymers. Figure S1 indicates that indeed the blend micelles are micelles that contain both parent polymers and are not a binary mixed solution.

$$N_{agg\ mix} = \frac{(C_1 N_{agg\ 1}) + (C_3 N_{agg\ 3})}{(C_1 + C_3)} \quad (S8)$$

$$R_h\ mix = \frac{(C_1 M_w\ 1) + (C_3 M_w\ 3)}{\left(\frac{C_1 M_w\ 1}{R_{h1}} + \frac{C_3 M_w\ 3}{R_{h3}}\right)} \quad (S9)$$

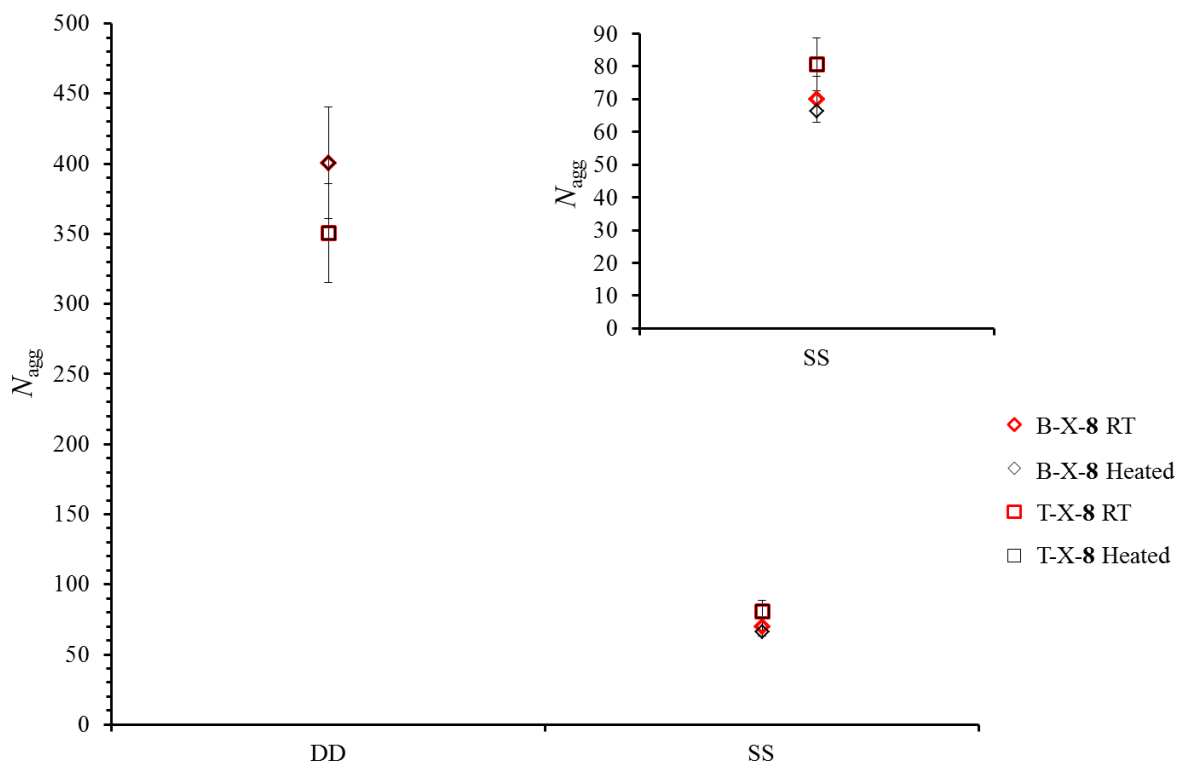


Figure S1. Relationship of N_{agg} with preparation pathway for the blended and pure solutions for the P(IBA-*co*-DMA)-*b*-PDMA diblock copolymers **8** at room temperature and after heating. Blend (B), theoretical (T) based on Eq. S8, X = Direct dissolution (DD), Solvent switch (SS). Error bars indicate 10% error on N_{agg} .

Variable temperature ^1H NMR spectroscopy

^1H NMR spectroscopy data shown in Figure S2 demonstrates the associating core block mobility. For these studies, increases in the intensity of the resonances that correspond to the associating core block demonstrate increased mobility. For this variable temperature ^1H NMR spectroscopy experiments B-DD-2 were explored. Here it could be observed that as the temperature increased the relative area of the peak at 0.8 ppm (representative of the EHA monomer) increased (Figure S2). Here a small increase in relative peak area was initially observed as temperature is increased but then a significantly larger increase in peak area was observed which subsequently plateaus at approximately 50-60 °C. It is understood that the

interaction of polymer chains with solvent is inversely proportional to the magnetic relaxation in ^1H NMR spectroscopy, specifically the relaxation is less for interacting polymer chains confined to the micelle core.¹⁰ Therefore it is hypothesised that a positive linear trend could be anticipated if polymer chains were not released by the micelle, as an increase in temperature could yield increased micelle solvent interactions in solution or possibly increased swelling of the micelle core with solvent resulting in faster magnetic relaxation.¹¹ Therefore, expulsion of a unimer chain from a micelle core would likely result in a much larger increase in proton signal intensity in ^1H NMR spectroscopy at a temperature and increased solvent polymer interactions in comparison to confined yet mobile polymer chains in the core.¹² Therefore, it was anticipated that a deviation from a linear trend would be observed for such phenomena. As such it is believed that the P(EHA-*co*-DMA)-*b*-PDMA diblock copolymer chains can possibly reorganise through the diffusion of unimers between micelles at high temperature. As the cores for the polymers studied are assumed to have minimal thermodynamic incompatibility with one another and the P(EHA-*co*-DMA)-*b*-PDMA diblock copolymers **1** and **3** can exchange at elevated temperature, blend micelles which structurally match pure micelles at the same composition of **2** can form.

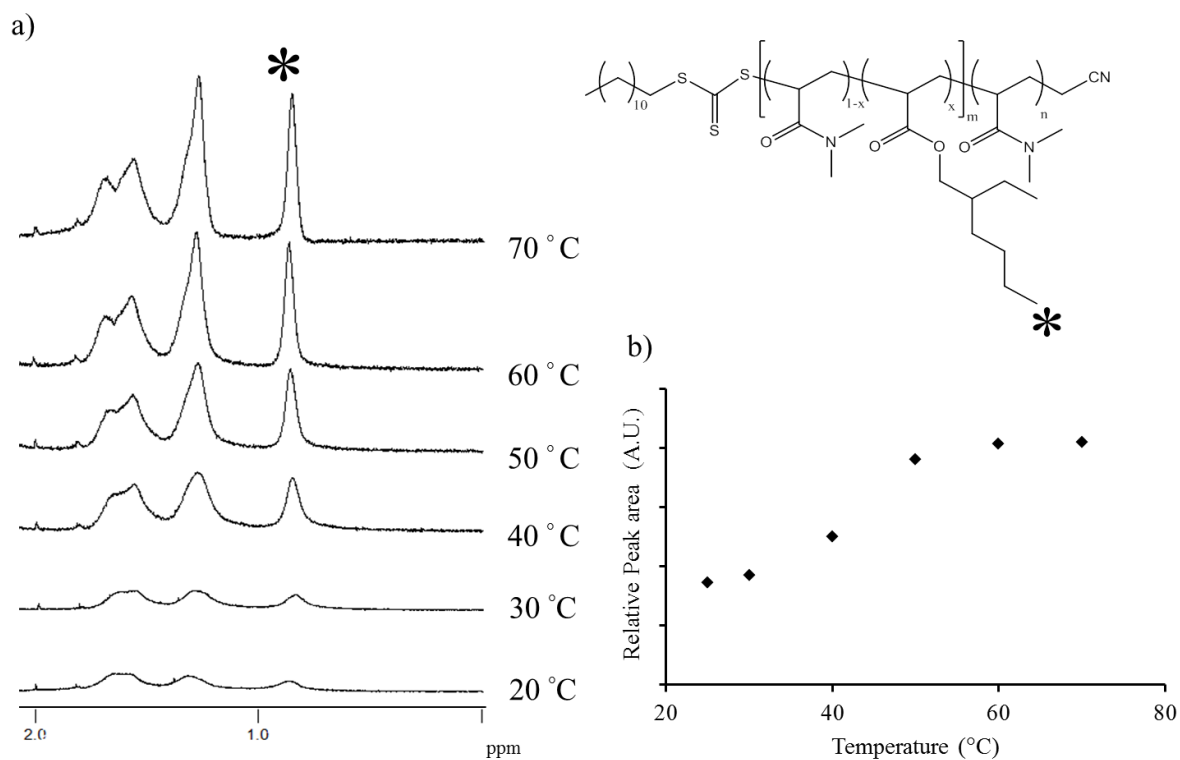


Figure S2. a) Partial ^1H NMR spectra for B-DD-2 upon gradual heating from 20 °C to 70 °C in D_2O . Data normalised to the solvent peak. b) Relationship between relative peak area at 0.8 ppm and temperature.

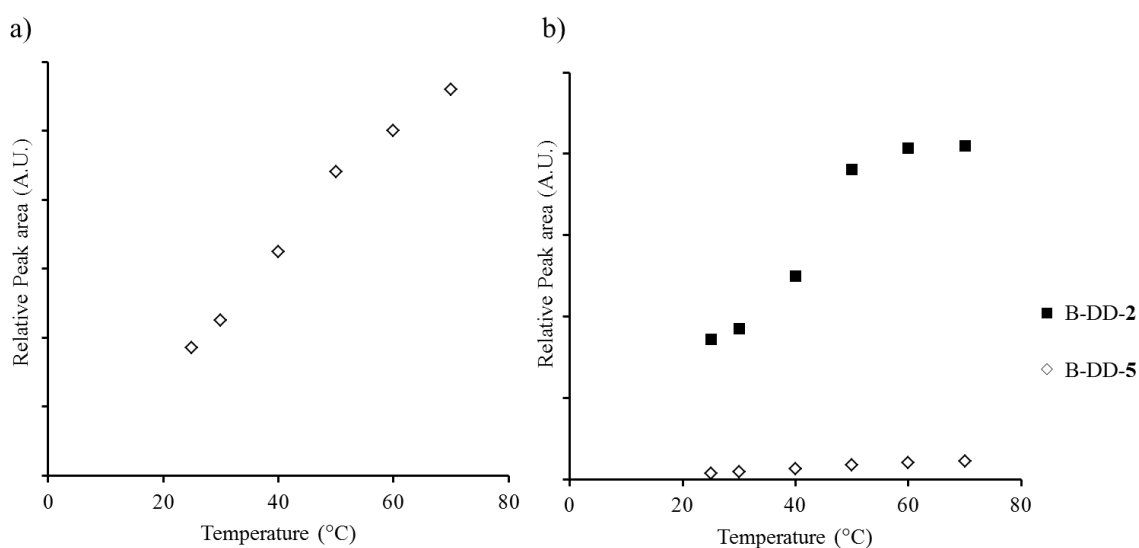


Figure S3. a) Relationship between relative peak area at 0.8 ppm from ^1H NMR spectroscopy and temperature for B-DD-5 upon gradual heating from 20 °C to 70 °C in D_2O . b)

Relationship between relative peak area at 0.8 ppm from ^1H NMR spectroscopy and temperature for B-DD-5 and B-DD-2 upon gradual heating from 20 °C to 70 °C in D_2O . Data normalised to solvent D_2O peak.

When the relative peak area of B-DD-5 was compared to B-DD-2 a large difference in the intensities is observed (Figure S3b). For the B-DD-5 system, the relative peak area was much smaller than those for B-DD-2 studies which indicated reduced polymer solvent interactions and consequently a reduced mobility for the B-DD-5 system.

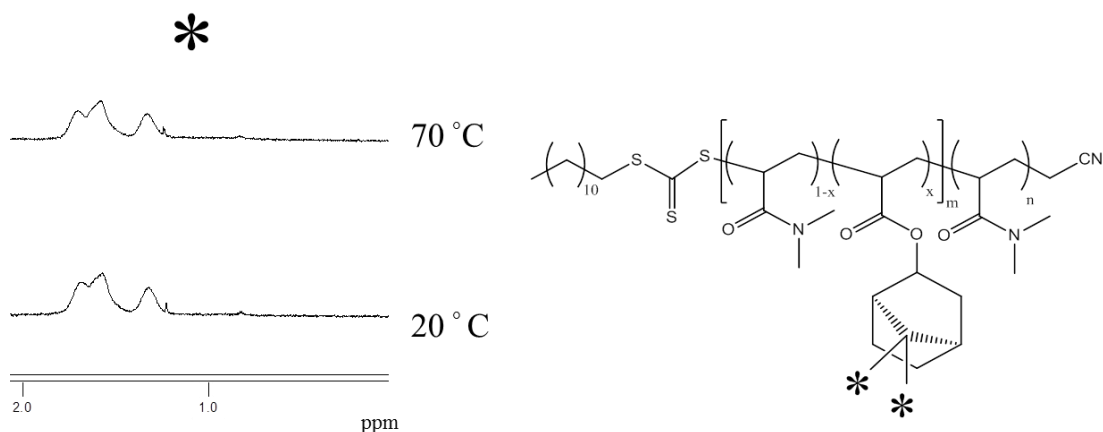


Figure S4. Partial ^1H NMR spectra for P(IBA-*co*-DMA)-*b*-PDMA diblock copolymers, B-SS-8, at 20 °C and 70 °C in D_2O . Expected ppm for asterix protons is 0.9-1.0. Data normalised to D_2O solvent peak.

^1H NMR spectroscopy of the signals attributed to the core block methyl protons from polymer **8** cannot be observed at room temperature or at 70 °C studied herein (Figure S4). This phenomenon leads to the conclusion that there was restricted mobility of the core and that the core block never resides in the solvent or solvent does not penetrate the micelle core.

Dynamic light scattering of blends formed from 5.

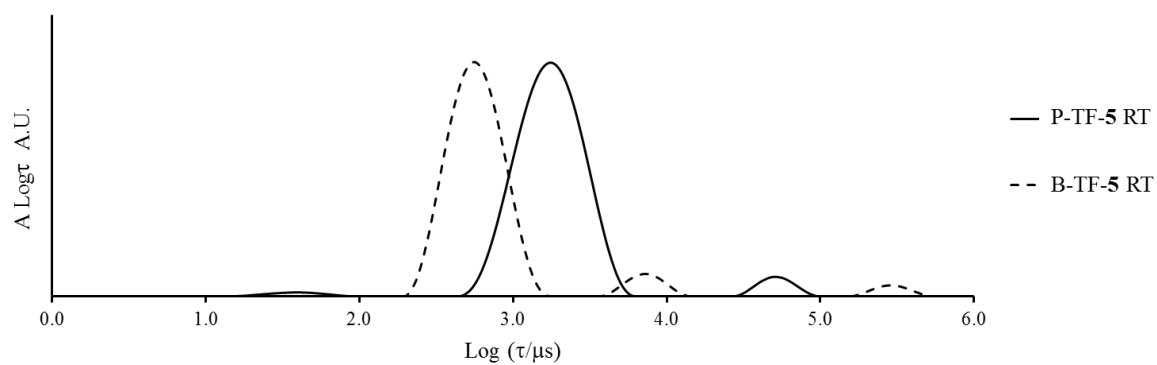


Figure S5. Example distributions of relaxation times from DLS for P(EHA-*co*-DMA)-*b*-PDMA blended and pure by thin film rehydration. Note the multiple populations in each sample.

Cryo-TEM analysis of 8

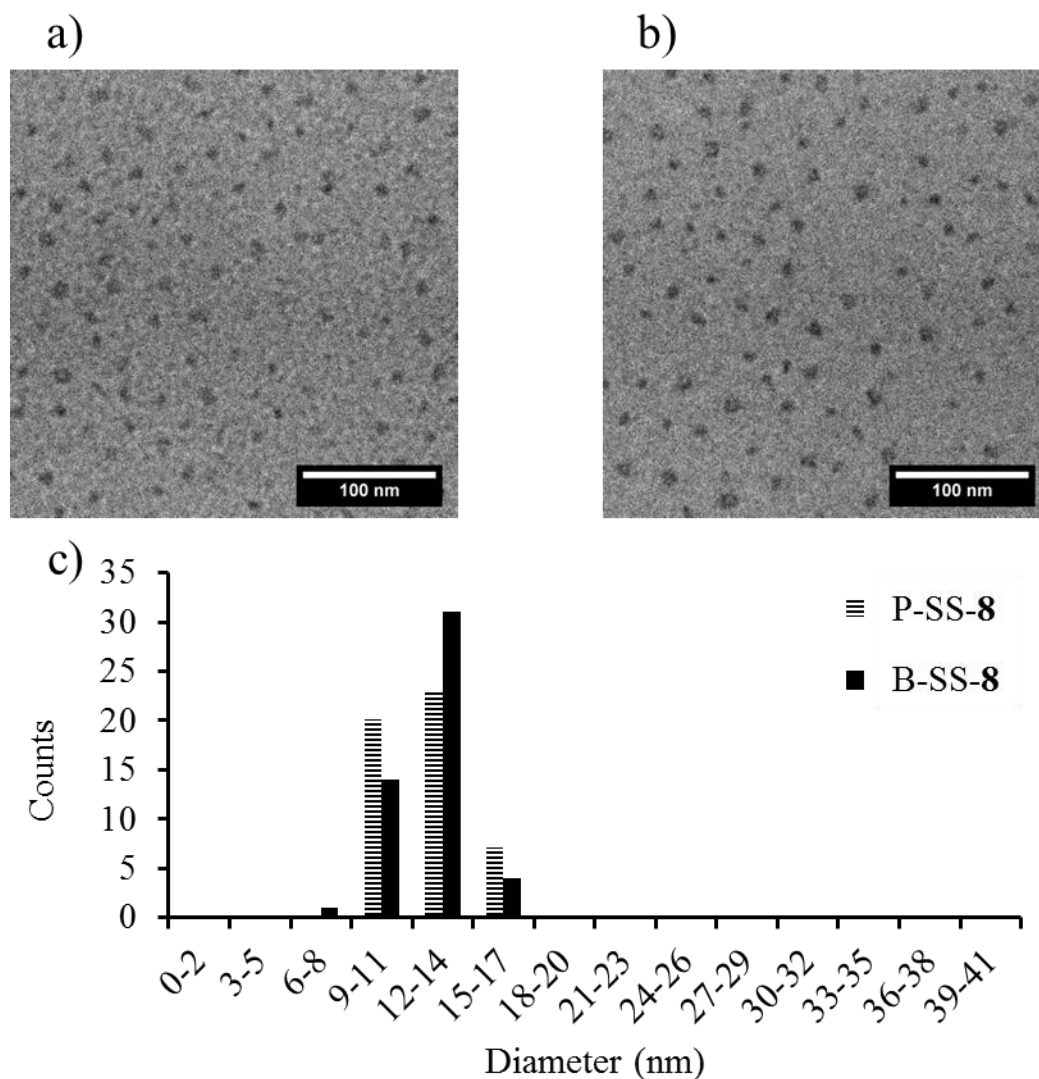


Figure S6. a) Cryo-TEM micrograph for the P-SS-8 after heating. b) cryo-TEM micrograph for B-SS-8 after heating. c) Histogram of core diameter for blended micelles from P-SS-8 and B-SS-8 (averaged over 50 particles).

REFERENCES

- 1 Jakes, J. *Collection of Czechoslovak Chemical Communications* **1995**, 60, 1781.
- 2 Nicolai, T.; Gimel, J. C.; Johnsen, R. *J. Phys. II* **1996**, 6, 695.
- 3 Chassenieux, C.; Nicolai, T.; Durand, D. *Macromolecules* **1997**, 30, 4952.
- 4 Sedlak, M. *J. Chem. Phys.* **1997**, 107, 10805.
- 5 Sedlak, M. *J. Chem. Phys.* **1997**, 107, 10799.
- 6 Yang, T. P.; Pearce, E. M.; Kwei, T. K.; Yang, N. L. *Macromolecules* **1989**, 22, 1813.

- 7 Plessis, C.; Arzamendi, G.; Alberdi, J. M.; Agnely, M.; Leiza, J. R.; Asua, J. M. *Macromolecules* **2001**, *34*, 6138.
- 8 Jakubowski, W.; Juhari, A.; Best, A.; Koynov, K.; Pakula, T.; Matyjaszewski, K. *Polymer* **2008**, *49*, 1567.
- 9 Hayward, R. C.; Pochan, D. J. *Macromolecules* **2010**, *43*, 3577.
- 10 Cheng, G.; Hammouda, B.; Perahia, D. *Macromol. Chem. Phys.* **2014**, *215*, 341.
- 11 Gowney, D. J.; Mykhaylyk, O. O.; Armes, S. P. *Langmuir* **2014**, *30*, 6047.
- 12 Hiller, W.; Engelhardt, N.; Kampmann, A.-L.; Degen, P.; Weberskirch, R. *Macromolecules* **2015**, *48*, 4032.